Langmuir

Article

pubs.acs.org/Langmuir

Synthesis and Physicochemical Characterization of Amphiphilic Triblock Copolymer Brush Containing pH-Sensitive Linkage for Oral Drug Delivery

You Qiang Yang, Wen Jing Lin, Bin Zhao, Xiu Fang Wen, Xin Dong Guo, and Li Juan Zhang*

School of Chemistry and Chemical Engineering, South China University of Technology, Guangzhou, 510640, P. R. China

ABSTRACT: A novel and well-defined pH-sensitive amphiphilic triblock copolymer brush poly(lactide)-*b*-poly(methacrylic acid)-*b*-poly(poly(ethylene glycol) methyl ether monomethacrylate) (PLA-*b*-PMAA-*b*-PPEGMA) and its self-assembled micelles were developed for oral administration of hydrophobic drugs. The copolymer and its precursors were synthesized by the combination of activators regenerated by electron transfer atom transfer radical polymerization (ARGET ATRP) and ring-opening polymerization (ROP) techniques. The molecular structures and characteristics were confirmed by GPC, ^{1}H NMR, and FT-IR. The critical micelle concentration (CMC) values of PLA-*b*-PMAA-*b*-PPEGMA in aqueous medium varied from 1.4 to 2.6 mg/L, and the partition equilibrium constant (K_v) of pyrene in micellar solutions ranged from 2.873×10^5 to 3.312×10^5. The average sizes of the self-assembled blank and drug-loaded micelles were 140−250 nm determined by DLS in aqueous solution. The morphology of the micelles was found to be spherical by SEM. Nifedipine (NFD), a poorly water-soluble drug, was selected as the model drug and wrapped into the core of micelles via dialysis method. The *in vitro* release behavior of NFD from the micelles was pH-dependent. In simulated gastric fluid (SGF, pH 1.2), the cumulative release percent of NFD was relative low, while in simulated intestinal fluid (SIF, pH 7.4), more than 96% was released within 24 h. All the results showed that the pH-sensitive PLA-*b*-PMAA-*b*-PPEGMA micelle may be a prospective candidate as oral drug delivery carrier for hydrophobic drugs with controlled release behavior.

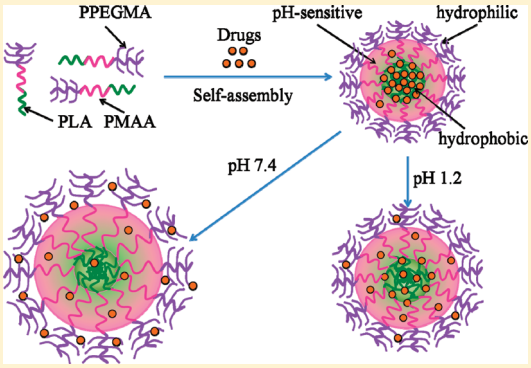

1. INTRODUCTION

Oral administration is one of the most common routes preferred by patients owing to its convenience, cost-effectiveness, flexibility in various chronic treatment regimes, and high level of patient acceptance.[1,2] However, when delivered orally, many hydrophobic drugs fail to arrive at their target sites through the gastrointestinal tract, which leads to low bioavailability, because of a lack of water solubility.[3,4] Polymeric core−shell micelles self-assembled from amphiphillic block copolymers have received much attention as drug carriers, due to their unique hydropholic inner core, which can enhance the loading efficiency and provide a desirable microenvironment for the incorporation of hydrophobic drugs.[5−8] Meanwhile, the outer hydrophilic shell can also provide a stable interface between the hydrophobic core and the aqueous environment besides compartmentalization of hydrophobic drugs. Appropriate micellar size (20−300 nm in diameter) and a lower critical micelle concentration (CMC) are important characteristics that can lead to higher biophysical stability, longer blood circulation time, lower toxic side effects, and prevention of recognition and uptake by the reticuloendothelial system (RES).[9−12]

An ever-increasing number of types of stimuli (pH, temperature, redox, light, ultrasound, and enzyme) are being explored on the environmentally sensitive micelles as smart drug delivery systems, and the pH-sensitivity is still one of the most extraordinary and significant methods.[13−16] The different pH-sensitive polymeric micelles as oral drug carriers can be designed to be a suitable release for different organs, tissues, and cells. A successful oral polymeric micellar vehicle should remain stable in the stomach (pH 1.0−3.0), which maintains in a closed form and prevents the release of drugs from the core of micelles, while releasing the molecularly dispersed drug in the intestine (pH 5.1−7.8), thereby preventing burst drug release and avoiding precipitation in the upper part of gastrointestinal tract.[17−21] Poly(acrylic acid) (PAA) and poly(methacrylic acid) (PMAA), bearing the carboxylic group with pK_a around 5−6, are the two representative and frequently pH-sensitive polymers used in oral DDS. They are commonly accepted as bioadhesive and safe polymers, as the ionic carboxyl of PAA or PMAA in the micellar corona can facilitate mucoadhesion. This enhances the residence time of the drug-entrapped micelles in the gastrointestinal tract and ensures complete drug dissolution, and eventually maximizes drug absorption in the small intestine.[22,23]

The objective of the current work is to design and synthesize a novel well-defined pH-sensitive amphiphilic triblock copolymer brush PLA-*b*-PMAA-*b*-PPEGMA and its self-assembled

Received: March 14, 2012
Revised: May 3, 2012
Published: May 8, 2012

dx.doi.org/10.1021/la301099q | *Langmuir* 2012, 28, 8251−8259

micelles for oral administration of hydrophobic drugs. The hydrophobic PLA block has been widely used in biomedical applications for its excellent biocompatibility and bioabsorbability *in vivo*.[24] It formed the micelle core, maintained high drug loading content and controlled the drug release rate. PMAA block was designed to be a block copolymer structure, which made the core more sensitive to the pH change of the environment when the polymer self-assembled into micelles. The hydrophilic PPEGMA with short side chains, known to be nonimmunogenic, nonantigenic and nontoxic, distributed on the surface of the self-assembled micelles, providing a compact steric protective layer to maintain the stability of micelles during biological circulation.[25] Nifedipine, a dihydropyridine calcium-channel blocker, has received much attention for its utility in the treatment of hypertension, angina, and myocardial infarction.[26] It is therefore desirable to develop nifedipine controlled-release chemotherapeutic agents to reduce the side effects, prevent toxicity, extend half-time, and improve patient compliance. Herein, nifedipine was used as the model drug and was encapsulated into PLA-*b*-PMAA-*b*-PPEGMA assembled micelles. The effect of the PMAA block length on the pH sensitivity of the nifedipine-loaded micelles was studied. Figure 1 shows the schematic micellization and pH-dependent drug release process of PLA-*b*-PMAA-*b*-PPEGMA in aqueous solution.

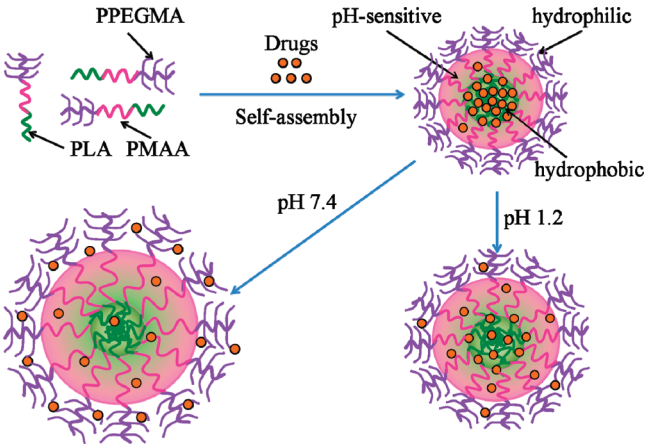

Figure 1. Scheme of drug loading and pH-dependent release from PLA-*b*-MAA-*b*-PPEGMA micelles.

2. EXPERIMENTAL SECTION

2.1. Materials. *tert*-Butyl methacrylate (*t*BMA, TCI-EP) were washed with sodium hydroxide solution (10%), distilled from calcium hydride, and stored under argon at −20 °C. D,L-Lactide (D,L-LA, Aldrich) was recrystallized from ethyl acetate three times and dried at room temperature under reduced pressure. PEGMA (M_n = 300 Da, Aldrich, 99%) was purified by passing through a column filled with neutral alumina to remove inhibitor. Dichloromethane (DCM, 99.8%, Sigma-Aldrich), triethylamine (TEA, 99%, Sigma-Aldrich), and toluene were dried over CaH_2 and distilled under nitrogen flow. Nifedipine (NFD, 99%, Sigma-Aldrich), pyrene (99%, Aldrich), ethyl 2-bromoisobutyrate (EBriB, 99%, Aldrich), *N*,*N*,*N*′,*N*′,*N*′-pentamethyl diethyl enetriamine (PMDETA, 99%, Aldrich), tetrahydrofuran (THF), trifluoroacetic acid (TFA), *n*-hexane, $CuBr_2$, methanol, acetone, and all other reagents were used as received.

2.2. Synthesis of Difuctional Initiator 2-Hydroxylethyl-2-Bromoisobutyrate (HEBriB). HEBriB was synthesized as follows:[27] To a flame-dried 150 mL Schlenk flask with a magnetic stirring bar, which was evacuated and flushed with argon three times, ethylene glycol (112 mL, 2 mol) and triethylamine (11.13 mL, 80 mmol) were introduced at 0 °C. Then, 2-bromopropionyl bromide (0.989 mL, 80 mmol) was added dropwise to the cold solution for a period of 2 h. The reaction was continued at 0 °C for 2 h and then heated to 40 °C for another 5 h. The reaction mixture was cooled, added to 500 mL of deionized water, and extracted with chloroform three times, and then the chloroform layer was washed successively with dilute HCl, saturated $NaHCO_3$, and water. The organic phase was dried through $MgSO_4$ overnight followed by rotary evaporation to remove the solvent. The colorless liquid product was collected by distillation under reduced pressure and characterized by ^{1}H NMR ($CDCl_3$, as solvent): $-C(CH_3)_2Br$ δ = 2.05 ppm (6H), CH_2-CH_2-OH δ = 3.85 ppm (2H), CH_2-CH_2-OH δ = 4.29 ppm (2H), CH_2-CH_2-OH δ = 2.33 ppm (1H).

2.3. ARGET ATRP of tBMA Initiated by HEBriB. Poly(*tert*-butyl methacrylate) (HO-P*t*BMA-Br) was synthesized by ARGET ATRP.[28,29] Typically, a previously dried 50 mL Schlenk flask equipped with a magnetic stirring bar was charged with $CuBr_2$ (11.2 mg, 0.05 mmol), and the flask was evacuated and flushed with argon three times. Anhydrous toluene (18 mL) and *t*BMA (5.715 mL, 35.2 mmol) were added to the flask using degassed syringes, and the mixture was homogenized by ultrasonic dispersion 10 min. Then, PMDETA (0.210 mL, 1 mmol) was introduced into the flask via syringe, and stirred 10 min until the Cu/PMDETA catalyst complex was formed. $Sn(Oct)_2$ (0.162 mL, 0.5 mmol) in toluene (2 mL) was then added to reduce the deactivator. Finally, HEBriB (0.165 mL, 1 mmol) was added and the flask was placed in a preheated oil bath maintained at 90 °C for 2 h. The flask was removed from the oil bath and cooled to room temperature. After the solvent was removed on a rotary evaporator, the reaction mixture was diluted with THF and passed through a neutral alumina column to remove the catalyst. Finally, HO-P*t*BMA-Br was precipitated by adding the solution into 10-fold excess of water/methanol (1:1, v/v) mixture, filtered, and dried under vacuum for 24 h.

2.4. ROP of D,L-LA in the Presence of HO-P*t*BMA-Br. Poly(lactide)-*b*-poly(*tert*-butylmethacrylate) (PLA-*b*-P*t*BMA-Br) diblock copolymer was synthesized by ROP.[30,31] The freshly recrystallized momomer D,L-LA (2.5 g, 0.5 mmol) and macroinitiator HO-P*t*BMA-Br (M_n = 4549, 0.5 mmol) were placed in a flame-dried 50 mL Schlenk flask with a magnetic stirring bar, and the Schlenk flask was evacuated and backfilled with argon three times. Subsequently, a required amount of $Sn(Oct)_2$ (0.081 mL, 0.5 mmol) in toluene (20 mL) was added, and three freeze−pump−thaw cycles were performed to remove any oxygen from the solution. The flask was filled with argon and placed into a thermostatted oil bath at 100 °C for 24 h. Afterward, the flask was removed from the oil bath and cooled to a room temperature followed by rotary evaporation to remove the solvent. The crude polymer was dissolved in approximately 30 mL THF and added dropwise to 300 mL water/methanol (1:1, v/v) mixture to precipitate the product, which was collected and dried under vacuum for 24 h.

2.5. Synthesis of PLA-*b*-P*t*BMA-*b*-PPEGMA. The synthetic procedure of poly(lactide)-*b*-poly(*tert*-butyl methacrylate)-*b*-poly(poly(ethylene glycol) methyl ether monomethacrylate) (PLA-*b*-P*t*BMA-*b*-PPEGMA) is similar to that of HO-P*t*BMA-Br. Briefly, a previously dried 50 mL Schlenk flask equipped with a magnetic stirring bar was charged with PLA-*b*-P*t*BMA-Br (M_n = 6516, 0.6 mmol) and $CuBr_2$ (6.7 mg, 0.03 mmol). After three degassed and backfilled cycles with argon, anhydrous toluene (18 mL), macromonomer PEGMA (0.343 mL, 12 mmol), and PMDETA (0.063 mL, 0.3 mmol) were injected into the reaction flask with syringe. After stirring for 15 min, a solution of $Sn(Oct)_2$ (0.097 mL, 0.3 mmol) in toluene (2 mL) was added and three freeze−pump−thaw cycles were conducted. The flask was transferred into a thermostatted oil bath at 70 °C for 24 h. After the solvent was removed on a rotary evaporator, the reaction mixture was diluted with THF, passed through a neutral alumina column, and precipitated with *n*-hexane. The final dried powder products were obtained after vacuum drying for 24 h.

2.6. Hydrolysis of PLA-*b*-P*t*BMA-*b*-PPEGMA. Poly(lactide)-*b*-poly(methacrylic acid)-*b*-poly(poly(ethylene glycol) methyl ether

Scheme 1. Synthetic Route of PLA-*b*-PMAA-*b*-PPEGMA Copolymer

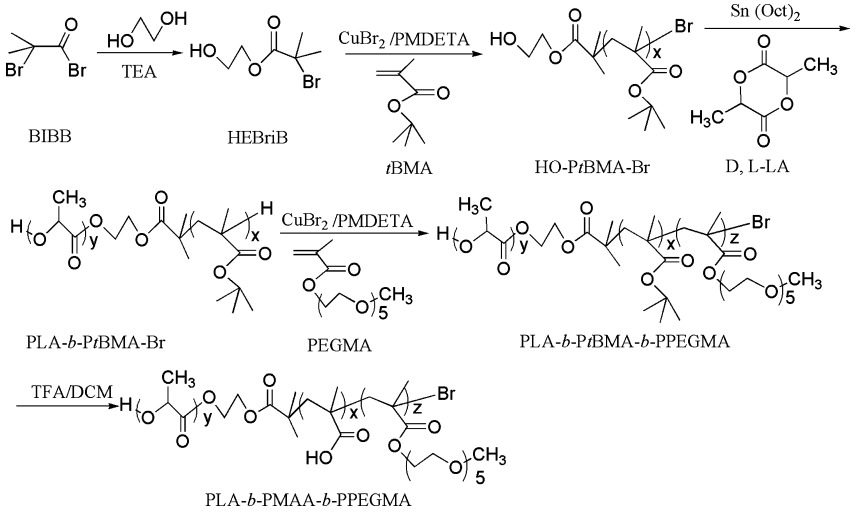

monomethacrylate) (PLA-*b*-PMAA-*b*-PPEGMA) was prepared by a selective hydrolysis of PLA-*b*-P*t*BMA-*b*-PPEGMA to remove the *tert*-butyl groups from P*t*BMA unit. In a typical experiment, 1500 mg of PLA-*b*-P*t*BMA-*b*-PPEGMA (M_n = 7276, 0.12 mmol) was dissolved in 15 mL of DCM. After cooling to 0 °C with ice/water bath, 2.64 mL of TFA (5-fold molar of *tert*-butyl groups) was slowly added with vigorous stirring. The mixture was stirred at 0 °C for 30 min and then carried out at room temperature for 4 h. After evaporating and removing all the solvents by rotary evaporation, the residues were dissolved in 5 mL of THF and precipitated into 50 mL of *n*-hexane (10-fold of THF) three times. The resulting brush-like copolymer PLA-*b*-PMAA-*b*-PPEGMA was collected by filtration and dried in a vacuum oven at 40 °C for 48 h.

2.7. Determination of Critical Micelle Concentrations (CMC). The formation of micelles self-assembled from PLA-*b*-PMAA-*b*-PPEGMA brush in an aqueous phase was confirmed by the fluorescence technique with a pyrene probe. The fluorescence of pyrene is well-known to be sensitive to change in the microenvironment. When the environment of pyrene changes from polar to nonpolar, the excitation spectra of pyrene are altered, and the peak shifts from 335 to 337 nm in the excitation spectra of pyrene as the copolymer concentration increases. In brief, the pyrene solution in acetone was added to deionized water (pH 6.5) until a pyrene concentration of 12×10^{-5} M was reached. Acetone was subsequently removed by rotary evaporator at 30 °C for 24 h. The final concentration of pyrene was adjusted to 6×10^{-7} M in the copolymer solution. The concentrations of polymer solution were varied from 0.0001 to 0.1 mg/mL. At last, the solutions were kept at room temperature in the dark for 24 h to reach the solubilization equilibrium between pyrene and copolymer.

2.8. Preparation of Blank and NFD-Loaded Micelles. The blank or NFD-loaded PLA-*b*-PMAA-*b*-PPEGMA micelles were prepared according to the diafiltration method. In a typical experiment, NFD (0−10 mg) and PLA-*b*-PMAA-*b*-PPEGMA (40 mg) were dissolved in 40 mL of DMF and stirred for 4 h at room temperature, followed by dialysis against deionized water (pH 6.5) for 24 h at 20 °C using a dialysis bag (molecular weight cutoff, MWCO 3500−4000). The deionized water was changed every 2 h for the first 6 h and then replaced every 6 h. After dialysis, half of the blank micelle solution was used to study the pH-responsive behavior of the micelle solution by the addition of NaOH or HCl (0.01 M) solution, and the remaining blank and NFD-loaded micelles were filtered by a membrane filter (0.45 μm pore) to remove aggregated particles and collected by freeze−drying to obtain dried product. The received white powder was stored at −20 °C until further experiments.

NFD loading content (LC) and entrapment efficiency (EE) were determined by UV−vis spectrophotometer (UV-2450, Shimadzu, Japan). One milligram of the NFD-loaded micelle powder was dissolved in 10 mL of ethanol under vigorous vortexing. The concentration of NFD at 237 nm was recorded with reference to a calibration curve of pure NFD/ethanol solution. The LC and EE of NFD were calculated using the following formulas 1 and 2, respectively. All samples were analysized in triplicate.

$$\mathrm{LC}(\%) = \frac{\text{weight of NFD-loaded drug}}{\text{weight of total polymer and drug in feed}} \times 100\% \quad (1)$$

$$\mathrm{EE}(\%) = \frac{\text{weight of NFD-loaded drug}}{\text{weight of NFD in feed}} \times 100\% \quad (2)$$

2.9. *In Vitro* Release of NFD from Micelles. The *in vitro* NFD release properties from the PLA-*b*-PMAA-*b*-PPEGMA assembled micelles were determined as follows: 5 mg of NFD-entrapped micelle was suspended in 3 mL of simulated gastric fluid (SGF, 0.15 M HCl, 0.05 M KCl, pH 1.2) or simulated intestinal fluid (SIF, 8 g NaCl, 0.2 g KCl, 1.44 g Na_2HPO_4, 0.24 g KH_2PO_4, 1 L water, pH 7.4) and then placed in a pre-swollen cellulose membrane bag (MWCO 3500−4000). The whole bag then was immersed into 30 mL of SGF or SIF buffer and shaken in a 37 °C water bath (Dissolution Tester RCZ-8B, TDTF, China) at 100 rpm. At specified time intervals, a 3 mL (V_e) sample was taken out and replaced by 3 mL fresh buffer to maintain the total volume. The concentrations of NFD in different samples were determined using UV−vis spectrophotometer. The cumulative drug release percent (E_r) was calculated based on the eq 3. The *in vitro* experiments were repeated three times, and all samples were analyzed in triplicate to get the final release curves.

$$E_r(\%) = \frac{V_e \sum_1^{n-1} C_i + V_0 C_n}{m_{\mathrm{NFD}}} \times 100 \quad (3)$$

where m_{NFD} represents the amount of NFD in the micelle (mg), V_0 is the whole volume of the release media (V_0 = 33 mL), and C_n represents the concentration of NFD in the *n*th sample (mg).

2.10. Characterization. The number average molecular weight (M_n) and polydispersity index (M_w/M_n) were determined by gel permeation chromatography (GPC) adopting an Agilent 1200 series GPC system equipped with a LC quant pump, PL gel 5 mm 500 Å, 10 000 Å, and 100 000 Å columns in series, and RI detector. The column system was calibrated with a set of monodisperse polystyrene standards using HPLC-grade THF as mobile phase with a flow rate of 1.0 mL/min at 30 °C.

^{1}H NMR spectra measurements were executed on a NMR spectrometer (Bruker AVANCE III 400, Switzerland) operating at 250 MHz, using deuterated chloroform ($CDCl_3$) or deuterated dimethyl sulfoxide (DMSO-d_6) as solvent and tetramethyl silane (TMS) as an internal standard. The temperature was 25 °C.

dx.doi.org/10.1021/la301099q | *Langmuir* 2012, 28, 8251−8259

Table 1. GPC and ^{1}H NMR Data of PLA-*b*-PMAA-*b*-PPEGMA Brushes and Its Precursors

entry	sample	$[M]_0/[I]_0$[a]	Con(%)[b]	DP[c]	$M_{n,NMR}$[c]	$M_{n,GPC}$[d]	M_w/M_n[d]
1	HO-P*t*BMA-Br$_1$	35:1	80.5	28.1	4216	4549	1.46
2	PLA-*b*-P*t*BMA-Br$_1$	40:1	39.4	15.8	6488	6516	1.48
3	PLA-*b*-P*t*BMA-*b*-PPEGMA$_1$	20:1	13.4	2.7	7291	7276	1.42
4	PLA-*b*-PMAA-*b*-PPEGMA brush$_1$	--	100	28.1	5708	5585	1.36
5	HO-P*t*BMA-Br$_2$	45:1	69.3	31.2	4643	4910	1.51
6	PLA-*b*-P*t*BMA-Br$_2$	40:1	43.0	18.8	7349	7160	1.46
7	PLA-*b*-P*t*BMA-*b*-PPEGMA$_2$	20:1	14.5	2.9	8218	8364	1.28
8	PLA-*b*-PMAA-*b*-PPEGMA brush$_2$	--	100	32.3	6566	6549	1.32

[a]Molar ratio of the initial monomer and initiator concentration. [b]Determined by ^{1}H NMR. [c]Calculated by ^{1}H NMR end group analysis. [d]Determined by GPC.

FT-IR spectra of PLA-*b*-PMAA-*b*-PPEGMA and its precursors were obtained in a transmission mode on a FT-IR spectrophotometer (Nicolet Nexus for Euro, America) under ambient condition. Samples were ground with KBr and then compressed into pellets. The spectra were taken from 400 to 4000 cm^{-1}. Typically, 32 scans at a resolution of 8 cm^{-1} were accumulated to obtain one spectrum.

Fluorescence spectra were obtained using a fluorescence spectrophotometer (F-4500, Hitachi, Japan) and the excitation spectra of polymer/pyrene solutions were scanned from 300 to 350 nm at room temperature, with an emission wavelength of 373 nm and bandwidth of 0.2 nm.

The micelle size (D_h) and distribution (PDI) were determined by dynamic light scattering (DLS, Malven Zetasizer Nano S, U.K.). The dialysis solutions were filtered through 0.45 μm pore size filters and the measurements were conducted in a 1.0 mL quartz cuvette, using a diode laser of 800 nm at 25 °C, and the scattering angle was fixed at 90°. The zeta potentials were determined by electrophoretic measurement carried out with the same Malven Zetasizer Nano S instrument and the measurements were performed three times for each sample at 25 °C. The D_h and zeta potential were received from the average of three measurement results.

Morphologies of blank and drug-loaded micelles were investigated by scanning electron microscopy (SEM, LEO 1530 VP, Germany). The sample was fixed on an aluminum stub as a thin film and coated with gold before observation. SEM was operated at an accelerating voltage of 5 kV and a magnification of 10 000× or 20 000× in the transmission electron mode.

3. RESULTS AND DISCUSSION

3.1. Synthesis and Characterization of the PLA-*b*-PMAA-*b*-PPEGMA Brush. PLA-*b*-PMAA-*b*-PPEGMA brush was synthesized via a combination of ARGET ATRP and ROP followed by selective hydrolysis of the *tert*-butyl groups of *t*BMA, as illustrated in Scheme 1. First, HEBriB was synthesized in the excess of ethylene glycol. Then, HEBriB was utilized as difunctional initiator for the ARGET ATRP of *t*BMA and subsequently ROP of D,L-LA to get PLA-*b*-P*t*BMA-Br. PLA-*b*-P*t*BMA-Br was then used to initiate the ARGET ATRP of PEGMA to form PLA-*b*-P*t*BMA-*b*-PPEGMA. Finally, PLA-*b*-PMAA-*b*-PPEGMA was harvested after the selective cleavage of the *tert*-butyl groups.

In the first-staged ARGET ATRP reaction, Cu/PMDETA complex was utilized as catalyst system. A sufficiently large excess of reducing agent $Sn(Oct)_2$ not only reduces Cu^{II} to Cu^{I} but is also responsible for scavenging oxygen and radical inhibitors. The monomer *t*BMA was polymerized in toluene at 90 °C with a conversion over 65% in 2 h and well-defined polymer with a narrow distribution on the condition that the molar ratio of $Sn(Oct)_2/CuBr_2$ was 10/1. By using hydroxy-terminated HO-P*t*BMA-Br as macroinitiator and $Sn(Oct)_2$ as catalyst, PLA-*b*-P*t*BMA-Br was synthesized through ROP of D,L-LA. The molar ratio HO-P*t*BMA-Br and D,L-LA was 40/1, which was carried out in toluene at 100 °C for 24 h. In the second-staged ARGET ATRP reaction, PLA-*b*-P*t*BMA-*b*-PPEGMA was prepared by using PLA-*b*-P*t*BMA-Br with bromoester terminal groups as macroinitiator. The reaction was carried out in toluene at 70 °C for 24 h in the presence of the same catalyst/ligand/reducing agent with HO-P*t*BMA-Br. The amphiphilic triblock PLA-*b*-P*t*BMA-*b*-PPEGMA was selectively hydrolyzed employing TFA as acid agent in DCM to acquire the target PLA-*b*-PMAA-*b*-PPEGMA brush, whose favorite reaction time of hydrolysis was 4 h.[32,33] With the hydrolysis underway, the numbers of *tert*-butyl groups were gradually reduced and the solution became turbid (slight yellow), in respect that PLA-*b*-PMAA-*b*-PPEGMA brush is insoluble in DCM.

The molecular weights of PLA-*b*-PMAA-*b*-PPEGMA brush and its precursors were determined by GPC and summarized in Table 1. The molar ratio of the initial monomer and initiator concentration from brush$_1$ and brush$_2$ were 35:1 and 45:1, respectively, resulting in different lengths of PMAA block, which affects the *in vitro* release behavior of the nifedipine-loaded micelles. Figure 2 (entries 1−4, Table 1) shows the

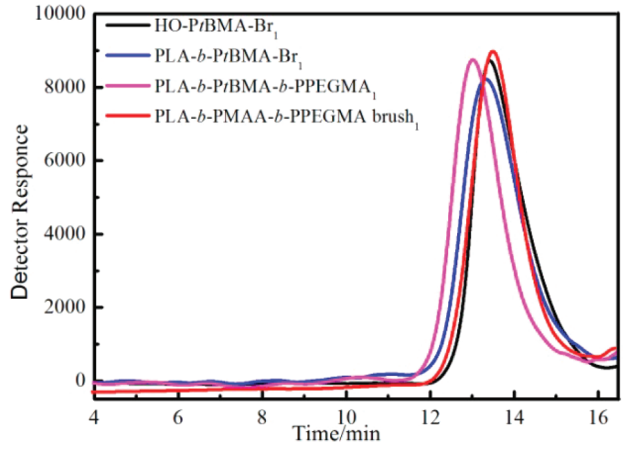

Figure 2. GPC traces of PLA-*b*-PMAA-*b*-PPEGMA brush$_1$ and its precursors.

GPC traces of the serial polymer products using the same HO-P*t*BMA-Br$_1$ macroinitiator. It can be seen that the resultant copolymers are shifted toward higher weight with increasing molecular weight of successive blocks (entries 1−3, Table 1 and Figure 2), while the molecular weight of the polymers decreases slightly after hydrolysis (entry 4, Table 1 and Figure 2). The molecular weights determined by GPC conformed to the

dx.doi.org/10.1021/la301099q | *Langmuir* 2012, 28, 8251−8259

theoretical values, and the M_w/M_n values were lower than 1.55 for the controlled/living polymerization.[34−36]

The chemical structures and formations of the products were further determined by ^{1}H NMR and FT-IR. The ^{1}H NMR spectra of PLA-*b*-PMAA-*b*-PPEGMA brush$_1$ (solvent, DMSO-d_6) and its percursors (solvent, $CDCl_3$) were depicted in Figure 3. In Figure 3A, the signals at 0.9−1.1, 1.42, and 1.7−1.9 ppm

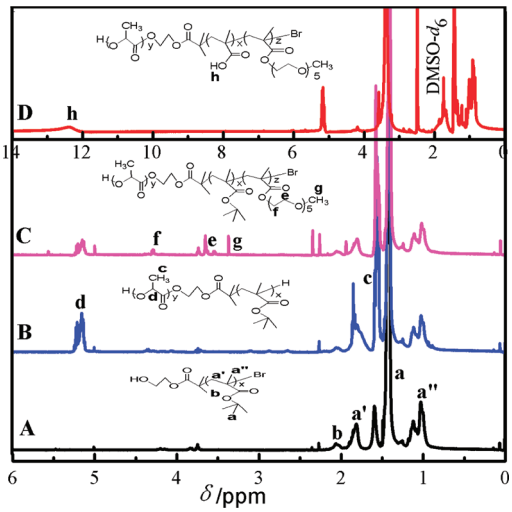

Figure 3. ^{1}H NMR spectra of HO-P*t*BMA-Br$_1$ (A), PLA-*b*-P*t*BMA-Br$_1$ (B), PLA-*b*-P*t*BMA-*b*-PPEGMA$_1$ (C), and PLA-*b*-PMAA-*b*-PPEGMA brush$_1$ (D).

are ascribed, respectively, to -C**H**$_3$, [-(C**H**$_3$)$_3$-], and -C**H**$_2$- in the *t*BMA unit, whereas the signals of -C**H**- and -C**H**$_3$- protons of PLA block can be found in peaks at 5.17 and 1.58 ppm (Figure 3B). As observed in Figure 3C, the characteristic PEGMA peaks at 3.28, 3.65, and 4.30 ppm due to -OC**H**$_3$, -OCH$_2$−C**H**$_2$O-, and -COO−C**H**$_2$- protons, respectively. After hydrolysis, the *tert*-butyl group (1.42 ppm) disappears while the carboxyl group (12.30 ppm) emerges, which can be seen in Figure 3D.

The degree of polymerization (DP) of P*t*BMA, PLA, and PPEGMA can be calculated from the ^{1}H NMR end group analysis according to the following formulas:[37,38]

$$DP_{PtBMA} = I_a/I_b \times 2/3 \quad (4)$$

$$DP_{PLA} = I_d/I_a \times 9 \times DP_{PtBMA} \quad (5)$$

$$DP_{PPEGMA} = I_e/I_d \times 1/10 \times DP_{PLA} \quad (6)$$

$$DP_{PMAA} = I_h/I_d \times DP_{PLA} \quad (7)$$

where I_a, I_b, I_d, I_e, and I_h are the intensities of the peaks at 1.42, 2.05, 5.17, 3.65, and 12.3 ppm, respectively.

The number-average molecular weights (M_n) can be thus obtained by the following equations:

$$M_{n(HO-PtBMA-Br)} = DP_{PtBMA} \times 142 + 211 \quad (8)$$

$$M_{n(PLA-b-PtBMA-Br)} = DP_{PLA} \times 144 + M_{n(HO-PtBMA-Br)} \quad (9)$$

$$M_{n(PLA-b-PtBMA-b-PPEGMA)} = DP_{PPEGMA} \times 300 + M_{n(PLA-b-PtBMA-Br)} \quad (10)$$

$$M_{n(PLA-b-PMAA-b-PPEGMA)} = DP_{PMAA} \times 86 + DP_{PLA} \times 144 + DP_{PPEGMA} \times 300 + 211 \quad (11)$$

The evidence of ^{1}H NMR spectra reported in Table 1 is in good agreement with the GPC values, indicating good control of the polymerization and preparation of well-defined copolymers.

As exhibit in the FT-IR spectra, the absorbance of -OH, C—H, C═O, and [-(CH$_3$)$_3$-] with stretching and bending bands in HO-P*t*BMA-Br (Figure 4A) occurs at 3446 cm^{-1}, 2979 cm^{-1},

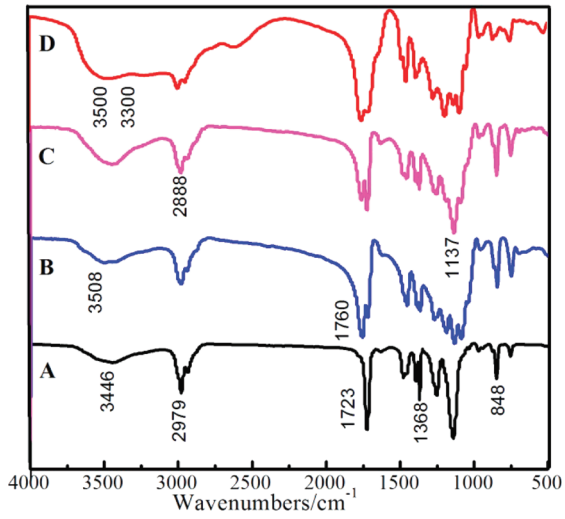

Figure 4. FT-IR spectra of HO-P*t*BMA-Br$_1$ (A), PLA-*b*-P*t*BMA-Br$_1$ (B), PLA-*b*-P*t*BMA-*b*-PPEGMA$_1$ (C), and PLA-*b*-PMAA-*b*-PPEGMA brush$_1$ (D).

1723 cm^{-1}, 1368 cm^{-1}, and 848 cm^{-1}, respectively. Furthermore, when the ring D,L-LA opens, stretching vibration are clearly observed at 3508 cm^{-1} and 1760 cm^{-1}, which are attributed to the PLA -OH and C═O stretching bands (Figure 4B). As Figure 4C shows, the characteristic PEGMA stretching vibration of C−H and C−O- are observed at 2888 cm^{-1} and 1137 cm^{-1}. For Figure 4A and C, the band ascribed to the C═C are not detected at 1640 cm^{-1}, supporting the formation of HO-P*t*BMA-Br and PLA-*b*-P*t*BMA-*b*-PPEGMA.[39,40] A broad absorption band with a characteristic range of 3300−3500 cm^{-1} is the stretching vibration of −OH in a carboxylic acid group, which reflects the hydrolysis of the *t*BMA (Figure 4D).

3.2. CMC Value of PLA-*b*-PMAA-*b*-PPEGMA Brush. CMC value of PLA-*b*-PMAA-*b*-PPEGMA and the hydrophobicity of the hydrophobic microdomain of the self-assembled micelles were determined by the fluorescence probe technique using pyrene as a fluorescence probe.[41,42] The CMC value was determined from the threshold concentration, where the intensity ratio I_{337}/I_{335} begins to increase markedly. The CMCs of PLA-*b*-PMAA-*b*-PPEGMA brush$_1$ and PLA-*b*-PMAA-*b*-PPEGMA brush$_2$ given in Figure 5 were determined to be 2.6 and 1.4 mg/L, respectively, which decreased with an increasing amount of hydrophobic PLA block, and results were summarized in Table 2. The results showed that a strong tendency for the copolymers bearing longer hydrophobic block to be prone to formation of micelles in aqueous solution. The CMCs of two copolymers were much lower than those of common surfactant, suggesting that the

dx.doi.org/10.1021/la301099q | *Langmuir* 2012, 28, 8251−8259

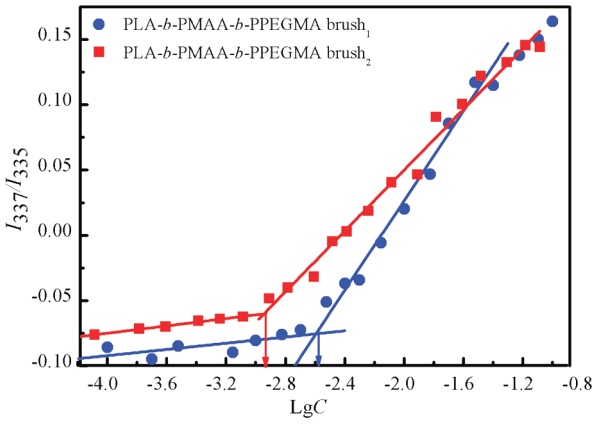

Figure 5. Plot of I_{337}/I_{335} ratios as a function of logarithm of PLA-*b*-PMAA-*b*-PPEGMA concentrations.

Table 2. Composition, CMC, and K_v of the Copolymers

sample	x_{PLA}[a]	x_{PPEGMA}[a]	x_{PMAA}[a]	CMC (mg/L)	K_v ($\times 10^5$)
PLA-*b*-PMAA-*b*-PPEGMA brush$_1$	0.398	0.141	0.424	2.6	2.873
PLA-*b*-PMAA-*b*-PPEGMA brush$_2$	0.412	0.132	0.425	1.4	3.312

[a]Determined by ^{1}H NMR.

micelles formed from PLA-*b*-PMAA-*b*-PPEGMA brush were relatively stable in solution, even after extreme dilution by the larger volume of systemic circulation in the body.[43]

The hydrophobicity of the inner core of self-aggregated micelles is one important factor in its application as a drug carrier. In this study, the partition equilibrium constant (K_v) of pyrene in the hydrophobic core of PLA-*b*-PMAA-*b*-PPEGMA brush micelles was calculated according to the method reported by Wilhelm et al.[44] and Kim et al.[45,46] This method calculates K_v based on the assumption of a simple equilibrium distribution between the micellar phase and the water phase. The method can be simplified as eq 12

$$(F - F_{min})/(F_{max} - F) = K_v x C/1000\rho \quad (12)$$

where F_{min} and F_{max} correspond to the average magnitude of the intensity ratio I_{337}/I_{335} in the flat region of low and high polymer concentration ranges, respectively, and F is the I_{337}/I_{335} in the intermediate concentration range in Figure 6. C is the concentration of PLA-*b*-PMAA-*b*-PPEGMA brush. x is the weight fraction of hydrophobic PLA in the brush, which is 0.398 and 0.412 for PLA-*b*-PMAA-*b*-PPEGMA brush$_1$ and PLA-*b*-PMAA-*b*-PPEGMA brush$_2$, respectively, shown in Table 2. ρ is the density of the PLA core of micelles, which is assumed to take the same value as bulk PLA (=1.25).[47] The K_v values for pyrene were obtained from the slope of the graph by plotting a graph of $(F - F_{min})/(F_{max} - F)$ versus the concentration of PLA-*b*-PMAA-*b*-PPEGMA brush as shown in Figure 6. Thus, the K_v values of brush$_1$ and brush$_2$ were determined to be 2.873 $\times 10^5$ and 3.312 $\times 10^5$ as summarized in Table 2. The effect of a longer hydrophobic PLA block is evident in the higher K_v, as a result, indicating the stronger hydrophobicity of the micellar cores. This is related to the hydrophilic/hydrophobic balance in the triblock copolymer, which consequently affects the micelle packing ability.

3.3. Characterization of the Blank and NFD-Loaded Micelles. All the blank and NFD-loaded PLA-*b*-PMAA-*b*-PPEGMA assembled micelles were prepared by diafiltration method against deionized water (pH 6.5). The size and size distribution (PDI) of the obtained blank and NFD-loaded micelles were measured by DLS, and the results are shown in Table 3. The size of blank micelle was about 140 nm and increased slightly to be about 150 nm after being loaded with NFD for PLA-*b*-PMAA-*b*-PPEGMA brush$_1$ (entries 1−4, Table 3). For PLA-*b*-PMAA-*b*-PPEGMA brush$_2$, the size increased from 214 to 250 nm after being entrapped with NFD (entries 5−8, Table 3). The NFD-loaded micelles showed a larger size than the blank micelles, which suggested that NFD was incorporated into the micelles effectively. The micelles maintained a narrow unimodal distribution, with a PDI between 0.200 and 0.400, suggesting a good physical performance of the assembled micelles.

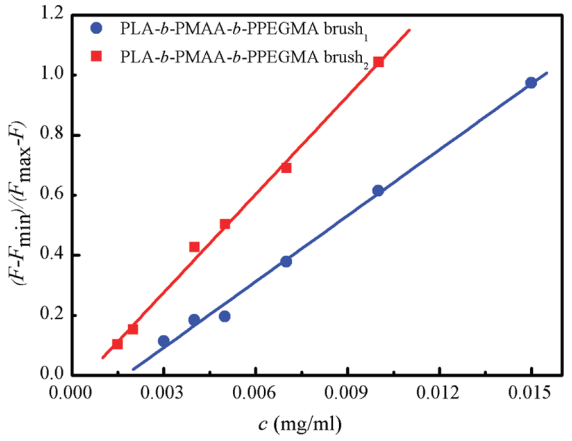

Figure 6. Plot of $(F - F_{min})/(F_{max} - F)$ vs concentration of PLA-*b*-PMAA-*b*-PPEGMA brushes in aqueous solution.

Zeta-potential measurement was used to further investigate the properties of the micelles. The blank and NFD-loaded micelles possess negative charges (−15 to −25 mV) due to COO^- groups in the PMAA chains and the potential is proportional to the amount of PMAA in the micelles (Table 3). These results suggested that the PLA-*b*-PMAA-*b*-PPEGMA brush micelles could be mucoadhesive, which facilitates the bioadhesion between the micelle carriers and intestinal epithelial cells.[48]

The variations of the size and zeta potential of the blank micelles as a function of pH were studied, as shown in Table 4. At higher pH above 6.3, the sizes of the micelles were increased because the PMAA segments protonated gradually, resulting in the increasing of hydrophilicity of PMAA and the swelling of the micelle. As can be also seen in Table 4, the zeta potential of the micelles presented higher negative charges when pH was above 6.3. When the pH values were between 6.3 and 4.5, the sizes were relative small due to the compact micelle structure assigned to PMAA segments deprotonated. However, the sizes increased sharply with pH decreasing below 2; this may be due to the fact that the micelles start to aggregate because of strong deionization of the micelles and intermolecular hydrogen bond formation.[49]

The morphology of the micelles was further examined using SEM. Figure 7 showed the SEM images of NFD-loaded PLA-*b*-PMAA-*b*-PPEGMA micelles, which demonstrated that the micelles were spherical in shape. It is of importance to note that the average sizes shown in SEM images were nearly consistent with the DLS results.

dx.doi.org/10.1021/la301099q | *Langmuir* 2012, 28, 8251−8259

Table 3. Size, Size Distribution, Zeta Potential, LC, and EE of NFD-Loaded Micelles

entry	polymer (mg)	NFD (mg)	feed ratio (%)	size (nm)	PDI	zeta potential (mV)	LC (%)	EE (%)
1	40[a]	0	0	140	0.389	−22.0	--	--
2	40[a]	6	15	151	0.417	−24.6	4.61	32.25
3	40[a]	8	20	141	0.436	−19.5	5.48	28.99
4	40[a]	10	25	155	0.431	−23.7	5.62	23.84
5	40[b]	0	0	214	0.238	−17.4	--	--
6	40[b]	6	15	233	0.232	−19.1	5.03	35.27
7	40[b]	8	20	257	0.280	−19.0	6.07	32.30
8	40[b]	10	25	237	0.348	−19.2	6.84	29.36

[a]PLA-*b*-MAA-*b*-PPEGMA brush$_1$. [b]PLA-*b*-MAA-*b*-PPEGMA brush$_2$.

Table 4. Size and Zeta Potential of PLA-*b*-PMAA-*b*-PPEGMA Micelles As a Function of pH

	PLA-*b*-MAA-*b*-PPEGMA brush$_1$				PLA-*b*-MAA-*b*-PPEGMA brush$_2$		
pH	size (nm)	PDI	zeta potential (mV)	pH	size (nm)	PDI	zeta potential (mV)
8.73	194	0.389	−25.1	8.62	238	0.283	−27.6
7.44	188	0.416	−24.6	7.42	231	0.233	−22.5
6.30	136	0.402	−21.6	6.35	209	0.261	−17.1
5.42	132	0.220	−20.2	5.56	203	0.312	−16.4
4.46	129	0.361	−18.3	4.60	184	0.129	−13.0
3.53	208	0.413	−13.2	3.48	216	0.226	−10.1
2.42	343	0.148	−2.8	2.33	385	0.325	−3.6
1.46	611	--	--	1.41	708	--	--

The LC and EE values of NFD-loaded micelles were illustrated in Table 3. It can be seen that weight ratios of drug to polymer had a profound influence on the LC and EE,[13] the LC increased with the increase of drug fed for both PLA-*b*-PMAA-*b*-PPEGMA brush micelles. Also, as for the same drug/polymer ratio, the copolymer micelles with longer-length PLA block and higher K_v exhibited enhanced drug entrapping ability. The larger the core of micelle assembled from more hydrophobic PLA content, the larger the amounts of drug that could be encapsulated into copolymer, which resulted in an increased LC. As for EE, an increase in the feed amount of NFD decreased its EE. It may be due to a strong interaction between the drug and the micelle core. In this case, the solubilization capacity may increase to a saturation level with increasing drugs. As a result, the EE in the micelles will decrease.[50,51]

3.4. *In Vitro* Release of NFD from PLA-*b*-PMAA-*b*-PPEGMA Brush Micelles. The release behavior of NFD at the fixed amount of drug (entries 4 and 8, Table 3) from the micelles with different lengths of PMAA block were evaluated at 37 °C in SGF (pH 1.2) and SIF (pH 7.4), as shown in Figure 8. For both brushes, the release rate was relatively low at acidic

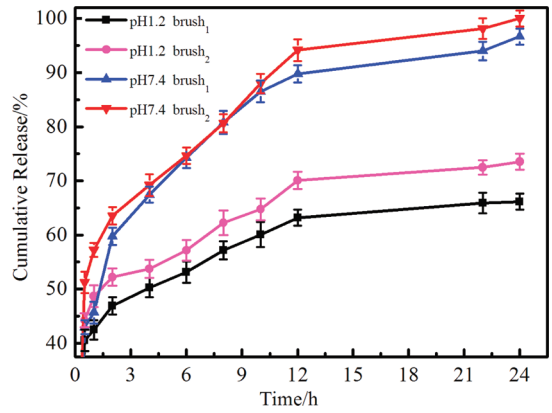

Figure 8. *In vitro* drug release profiles of NFD-loaded PLA-*b*-PMAA-*b*-PPEGMA brush assembled micelles.

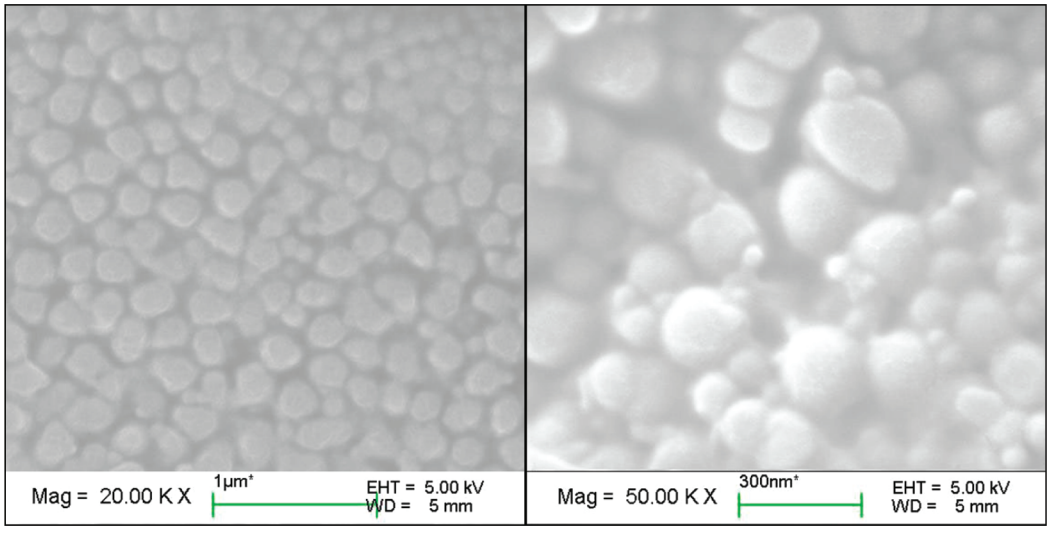

Figure 7. SEM images of NFD-loaded PLA-*b*-PMAA-*b*-PPEGMA brush$_1$ (A) and brush$_2$ (B) assembled micelles.

dx.doi.org/10.1021/la301099q | *Langmuir* 2012, 28, 8251−8259

pH (pH 1.2), with about 66−73% of NFD released after 24 h. On the other hand, the amount of NFD released accelerated significantly in the presence of pH 7.4; more than 96% of NFD was released within 24 h, due to the swelling of micelle structure caused by the stronger protonation of carboxyl groups of PMAA at higher pH conditions. The release rate of NFD was increased by improving the PMAA block ratio in the PLA-*b*-PMAA-*b*-PPEGMA. The cumulative release of PLA-*b*-PMAA-*b*-PPEGMA brush$_2$ micelle is higher (about 5%) than that of PLA-*b*-PMAA-*b*-PPEGMA brush$_1$ micelle in 12 and 24 h. Such a drug release pattern from the PLA-*b*-PMAA-*b*-PPEGMA micelles will ensure progressive and complete drug dissolution in the intestinal tract as well as maximize its release in the small intestine to offer the largest area for drug absorption, which can reduce the drug leakage in the stomach. The overall *in vitro* drug release results demonstrate that these pH-responsive micelles self-assembled from PLA-*b*-PMAA-*b*-PPEGMA show promise as delivery vehicles for the efficient administration of various hydrophobic drugs via the oral route. Encouraged by these promising results, further studies exploring better performance of pH-sensitive polymeric micelles by adjusting their molecular architecture are underway in our laboratory.

4. CONCLUSIONS

A novel pH-sensitive amphiphilic triblock copolymer PLA-*b*-PMAA-*b*-PPEGMA brush and its precursors were fabricated by combining of ARGET ATRP and ROP followed by hydrolysis of *tert*-butyl groups and characterized by GPC, ^{1}H NMR, and FT-IR. The results indicated that well-defined products with specific block length ratio and favorable M_w/M_n ($\cong$1.5) were acquired. The CMC values of PLA-*b*-PMAA-*b*-PPEGMA in aqueous medium were low (about 1−3 mg/L), suggesting a favorable stability of the assembled micelles. The values of K_v (2.873×10^5 to 3.312×10^5) suggested the potentially high encapsulation efficiency of hydrophobic drugs. The NFD-loaded micelles were 150−250 nm in size and spherical in shape. The *in vitro* release behavior of NFD from PLA-*b*-PMAA-*b*-PPEGMA micelles exhibited pH-dependence. In SGF (pH 1.2), the cumulative release percent of NFD was relatively low, while in SIF (pH 7.4), more than 96% of NFD was released within 24 h, which is desirable for oral delivery. These characteristics demonstrate that these PLA-*b*-PMAA-*b*-PPEGMA micelles could be employed as a promising vehicle for oral hydrophobic drug delivery. In addition, further increase of the molecular weight of PLA-*b*-PMAA-*b*-PPEGMA, as well as of the hydrophobic PLA block, may induce better control of drug release from micelles, especially in SGF conditions (pH 1.2), which is part of our ongoing work.

AUTHOR INFORMATION

Corresponding Author

*Tel/Fax: +86-20-87112046, E-mail: celjzh@scut.edu.cn.

Notes

The authors declare no competing financial interest.

ACKNOWLEDGMENTS

This work was financially supported by National Natural Science Foundation of China (No. 21176090), Team Project of Natural Science Foundation of Guangdong Province (No. S2011030001366), Guangzhou Municipal Bureau of Science and Technology (No. 2009J1-C511-2), the Fundamental Research Funds for the Central Universities (No. 2011ZM0041).

REFERENCES

(1) Le Lay, K.; Myon, E.; Hill, S.; Riou-Franca, L.; Scott, D.; Sidhu, M.; Dunlop, D.; Launois, R. Comparative Cost-Minimisation of Oral and Intravenous Chemotherapy for First-Line Treatment of Non-Small Cell Lung Cancer in the UK NHS System. *Eur. J. Health Econ.* **2007**, *8*, 145−151.

(2) Siew, A.; Le, H.; Thiovolet, M.; Gellert, P.; Schätzlein, A.; Uchegbu, I. Enhanced Oral Absorption of Hydrophobic and Hydrophilic Drugs Using Quaternary Ammonium Palmitoyl Glycol Chitosan Nanoparticles. *Mol. Pharmaceutics* **2012**, *9*, 14−28.

(3) Torchilin, V. P. Targeted Polymeric Micelles for Delivery of Poorly Soluble Drugs. *Cell. Mol. Life Sci.* **2004**, *61*, 2549−2559.

(4) Cho, K.; Wang, X.; Nie, S.; Shin, D. M. Therapeutic Nanoparticles for Drug Delivery in Cancer. *Clin. Cancer Res.* **2008**, *14*, 1310−1316.

(5) Tian, Y.; Ravi, P.; Bromberg, L.; Hatton, T. A.; Tam, K. C. Synthesis and Aggregation Behavior of Pluronic F87/Poly(acrylic acid) Block Copolymer in the Presence of Doxorubicin. *Langmuir* **2007**, *23*, 2638−2646.

(6) Hu, J.; Qian, Y.; Wang, X.; Liu, T.; Liu, S. Drug-Loaded and Superparamagnetic Iron Oxide Nanoparticle Surface Embedded Amphiphilic Block Copolymer Micelles for Integrated Chemotherapeutic Drug Delivery and MR Imaging. *Langmuir* **2012**, *28*, 2073−2082.

(7) Guo, X. D.; Zhang, L. J.; Chen, Y.; Qian, Y. Core/Shell pH-Sensitive Micelles Self-Assembled from Cholesterol Conjugated Oligopeptides for Anticancer Drug Delivery. *AIChE J.* **2010**, *56*, 1922−1931.

(8) Lee, S. J.; Min, K. H.; Lee, H. J.; Koo, A. N.; Rim, H. P.; Jeon, B. J.; Jeong, S. Y.; Heo, J. S.; Lee, S. C. Ketal Cross-Linked Poly(ethylene glycol)-Poly(amino acid)s Copolymer Micelles for Efficient Intracellular Delivery of Doxorubicin. *Biomacromolecules* **2011**, *12*, 1224−1233.

(9) Xiong, X. B.; Falamarzian, A.; Garg, S. M.; Lavasanifar, A. J. Engineering of Amphiphilic Block Copolymers for Polymeric Micellar Drug and Gene Delivery. *J. Controlled Release* **2011**, *155*, 248−261.

(10) Nelson-Mendez, A.; Aleksanian, S.; Oh, M.; Lim, H. S.; Oh, J. K. Reductively Degradable Polyester-Based Block Copolymers Prepared by Facile Polycondensation and ATRP: Synthesis, Degradation, and Aqueous Micellization. *Soft Matter* **2011**, *7*, 7441−7452.

(11) Zheng, H. T.; Ye, X. D.; Wang, H.; Yan, L. F.; Bai, R. K.; Hu, W. Q. A Facile One-Pot Strategy for Preparation of Small Polymer Nanoparticles by Self-Crosslinking of Amphiphilic Block Copolymers Containing Acyl Azide Groups in Aqueous Media. *Soft Matter* **2011**, *7*, 3956−3962.

(12) Yang, Y. Q.; Guo, X. D.; Lin, W. J.; Zhang, L. J.; Zhang, C. Y.; Qian, Y. Amphiphilic Copolymer Brush with Random pH-Sensitive/Hydrophobic Structure: Synthesis and Self-Assembled Micelles for Sustained Drug Delivery. *Soft Matter* **2012**, *8*, 454−464.

(13) Klaikherd, A.; Nagamani, C.; Thayumanavan, S. Multi-Stimuli Sensitive Amphiphilic Block Copolymer Assemblies. *J. Am. Chem. Soc.* **2009**, *131*, 4830−4838.

(14) Meng, F. H.; Zhong, Z. Y; Jan, F. J. Stimuli-Responsive Polymersomes for Programmed Drug Delivery. *Biomacromolecules* **2009**, *10*, 197−209.

(15) Roy, D.; Cambre, J. N.; Sumerlin, B. S. Future Perspectives and Recent Advances in Stimuli-Responsive Materials. *Prog. Polym. Sci.* **2010**, *35*, 278−301.

(16) Lin, W.; Kim, D. pH-Sensitive Micelles with Cross-Linked Cores Formed from Polyaspartamide Derivatives for Drug Delivery. *Langmuir* **2011**, *27*, 12090−12097.

(17) McDowell, A.; McLeod, B. J. Physiology and Pharmacology of the Brushtail Possum Gastrointestinal Tract: Relationship to the Human Gastrointestinal Tract. *Adv. Drug Delivery Rev.* **2007**, *59*, 1121−1132.

(18) Du, J. Z.; Tang, L. Y.; Song, W. J.; Shi, Y.; Wang, J. Evaluation of Polymeric Micelles from Brush Polymer with Poly(ε-caprolactone)-*b*-Poly(ethylene glycol) Side Chains as Drug Carrier. *Biomacromolecules* **2009**, *10*, 2169−2174.
(19) Tyrrell, Z. L.; Shen, Y.; Radosz, M. Fabrication of Micellar Nanoparticles for Drug Delivery through the Self-Assembly of Block Copolymers. *Prog. Polym. Sci.* **2010**, *35*, 1128−1143.
(20) Zhang, Y.; Li, X.; Zhou, Y.; Wang, X.; Fan, Y.; Huang, Y.; Liu, Y. Preparation and Evaluation of Poly(ethylene glycol)-Poly(lactide) Micelles as Nanocarriers for Oral Delivery of Cyclosporine A. *Nanoscale Res. Lett.* **2010**, *5*, 917−925.
(21) Negrini, R.; Mezzenga, R. pH-Responsive Lyotropic Liquid Crystals for Controlled Drug Delivery. *Langmuir* **2011**, *27*, 5296−5303.
(22) Lee, S. C.; Lee, H. J. pH-Controlled, Polymer-Mediated Assembly of Polymer Micelle Nanoparticles. *Langmuir* **2007**, *23*, 488−495.
(23) Lee, H. J.; Lee, S. C. Fabrication of Core-Shell Hybrid Nanoparticles by Mineralization on Poly(ε-caprolactone)-*b*-Poly-(methacrylic acid) Copolymer Micelles. *Polym. Bull.* **2010**, *65*, 743−752.
(24) Wu, Y.; Li, M. J.; Gao, H. X. Polymeric Micelle Composed of PLA and Chitosan as a Drug Carrier. *J. Polym. Res.* **2009**, *16*, 11−18.
(25) Hussain, H.; Mya, K. Y.; He, C. Self-Assembly of Brush-Like Poly[poly(ethylene glycol) methyl ether methacrylate] Synthesized via Aqueous Atom Transfer Radical Polymerization. *Langmuir* **2008**, *24*, 13279−13286.
(26) Buckley, N.; Dawson, A.; Whyte, I. Calcium Channel Blockers. *Medicine* **2007**, *35*, 599−602.
(27) Jakubowski, W.; Lutz, J. F.; Slomkowski, S.; Matyjaszewski, K. Block and Random Copolymers as Surfactants for Dispersion Polymerization. I. Synthesis via Atom Transfer Radical Polymerization and Ring-Opening Polymerization. *J. Polym. Sci., Part A: Polym. Chem.* **2005**, *43*, 1498−1510.
(28) Matyjaszewski, K.; Jakubowski, W.; Min, K.; Tang, W.; Huang, J.; Braunecker, W. A.; Tsarevsky, N. V. Diminishing Catalyst Concentration in Atom Transfer Radical Polymerization with Reducing Agents. *Proc. Natl. Acad. Sci. U.S.A.* **2006**, *103*, 15309−15314.
(29) Matyjaszewski, K.; Dong, H.; Jakubowski, W.; Pietrasik, J.; Kusumo, A. Grafting from Surfaces for "Everyone": ARGET ATRP in the Presence of Air. *Langmuir* **2007**, *23*, 4528−4531.
(30) Wolf, F. F.; Friedemann, N.; Frey, H. Poly(lactide)-*block*-Poly(HEMA) Block Copolymers: An Orthogonal One-Pot Combination of ROP and ATRP, Using a Bifunctional Initiator. *Macromolecules* **2009**, *42*, 5622−5628.
(31) Liu, J. Y.; Huang, W.; Pang, Y.; Zhu, X. Y.; Zhou, Y. F.; Yan, D. Y. Self-Assembled Micelles from an Amphiphilic Hyperbranched Copolymer with Polyphosphate Arms for Drug Delivery. *Langmuir* **2010**, *26*, 10585−10592.
(32) Li, Z.; Day, M.; Ding, J.; Faid, K. Synthesis and Characterization of Functional Methacrylate Copolymers and Their Application in Molecular Imprinting. *Macromolecules* **2005**, *38*, 2620−2625.
(33) Christodoulakis, K. E.; Vamvakaki, M. Amphoteric Core-Shell Microgels: Contraphilic Two-Compartment Colloidal Particles. *Langmuir* **2009**, *26*, 639−647.
(34) Braunecker, W. A.; Matyjaszewski, K. Controlled/Living Radical Polymerization: Features, Developments, and Perspectives. *Prog. Polym. Sci.* **2007**, *32*, 93−146.
(35) Wu, Z.; Chen, H.; Liu, X.; Zhang, Y.; Li, D.; Huang, H. Protein Adsorption on Poly(N-vinylpyrrolidone)-Modified Silicon Surfaces Prepared by Surface-Initiated Atom Transfer Radical Polymerization. *Langmuir* **2009**, *25*, 2900−2906.
(36) Magenau, A. J. D.; Strandwitz, N. C.; Gennaro, A.; Matyjaszewski, K. Electrochemically Mediated Atom Transfer Radical Polymerization. *Science* **2011**, *332*, 81−84.
(37) Zhu, W.; Nese, A.; Matyjaszewski, K. Thermoresponsive Star Triblock Copolymers by Combination of ROP and ATRP: From Micelles to Hydrogels. *J. Polym. Sci., Part A: Polym. Chem.* **2011**, *49*, 1942−1952.
(38) Zhang, W.; He, J.; Liu, Z.; Ni, P.; Zhu, X. Biocompatible and pH-Responsive Triblock Copolymer mPEG-*b*-PCL-*b*-PDMAEMA: Synthesis, Self-Assembly, and Application. *J. Polym. Sci., Part A: Polym. Chem.* **2010**, *48*, 1079−1091.
(39) Jang, J.; Ha, H. Fabrication of Hollow Polystyrene Nanospheres in Microemulsion Polymerization Using Triblock Copolymers. *Langmuir* **2002**, *18*, 5613−5618.
(40) Li, J.; Wang, Q.; Su, C.; Chen, Q. Preparation and Characterization of Fluorine-Containing Acrylate Copolymers by 60Co [gamma]-Ray Radiation Copolymerization. *Eur. Polym. J.* **2007**, *43*, 2928−2934.
(41) Kim, W.; Thévenot, J.; Ibarboure, E.; Lecommandoux, S.; Chaikof, E. L. Self-Assembly of Thermally Responsive Amphiphilic Diblock Copolypeptides into Spherical Micellar Nanoparticles. *Angew. Chem., Int. Ed.* **2010**, *49*, 4257−4260.
(42) Ren, T. B.; Feng, Y.; Zhang, Z. H.; Li, L.; Li, Y. Y. Shell-Sheddable Micelles Based on Star-Shaped Poly([varepsilon]-caprolactone)-SS-Poly(ethyl glycol) Copolymer for Intracellular Drug Release. *Soft Matter* **2011**, *7*, 2329−2331.
(43) Xue, Y. N.; Huang, Z. Z.; Zhang, J. T.; Liu, M.; Zhang, M.; Huang, S. W.; Zhuo, R. X. Synthesis and Self-Assembly of Amphiphilic Poly(acrylic acid-*b*-DL-lactide) to Form Micelles for pH-Responsive Drug Delivery. *Polymer* **2009**, *50*, 3706−3713.
(44) Wilhelm, M.; Zhao, C. L.; Wang, Y.; Xu, R.; Winnik, M. A.; Mura, J. L.; Riess, G.; Croucher, M. D. Poly(styrene-ethylene oxide) Block Copolymer Micelle Formation in Water: a Fluorescence Probe Study. *Macromolecules* **1991**, *24*, 1033−1040.
(45) Chang, Y.; Lee, S. C.; Kim, K. T.; Kim, C.; Reeves, S. D.; Allcock, H. R. Synthesis and Micellar Characterization of an Amphiphilic Diblock Copolyphosphazene. *Macromolecules* **2001**, *34*, 269−274.
(46) Kim, C.; Lee, S. C.; Shin, J. H.; Yoon, J. S.; Kwon, I. C.; Jeong, S. Y. Amphiphilic Diblock Copolymers Based on Poly(2-ethyl-2-oxazoline) and Poly(1, 3-trimethylene carbonate): Synthesis and Micellar Characteristics. *Macromolecules* **2000**, *33*, 7448−7452.
(47) Lee, C. T.; Huang, C. P.; Lee, Y. D. Preparation of Amphiphilic Poly(L-lactide)-*graft*-Chondroitin Sulfate Copolymer Self-Aggregates and Its Aggregation Behavior. *Biomacromolecules* **2006**, *7*, 1179−1186.
(48) Lo, C. L.; Lin, K. M.; Huang, C. K.; Hsiue, G. H. Self-Assembly of a Micelle Structure from Graft and Diblock Copolymers: An Example of Overcoming the Limitations of Polyions in Drug Delivery. *Adv. Funct. Mater.* **2006**, *16* (18), 2309−2316.
(49) Holappa, S.; Andersson, T.; Kantonen, L.; Plattner, P.; Tenhu, H. Soluble Polyelectrolyte Complexes Composed of Poly(ethylene oxide)-*block*-Poly(sodium methacrylate) and Poly-(methacryloyloxyethyl trimethylammonium chloride). *Polymer* **2003**, *44*, 7907−7916.
(50) Wang, F.; Bronich, T. K.; Kabanov, A. V.; Rauh, R. D.; Roovers, J. Synthesis and Characterization of Star Poly(ε-caprolactone)-*b*-Poly(ethylene glycol) and Poly(l-lactide)-*b*-Poly(ethylene glycol) Copolymers: Evaluation as Drug Delivery Carriers. *Bioconjugate Chem.* **2008**, *19* (7), 1423−1429.
(51) Thambi, T.; Deepagan, V.; Yoo, C. K.; Park, J. H. Synthesis and Physicochemical Characterization of Amphiphilic Block Copolymers Bearing Acid-Sensitive Orthoester Linkage as the Drug Carrier. *Polymer* **2011**, *52*, 4753−4759.